Meteoritics & Planetary Science 38, Nr 1, 81–94 (2003)
Abstract available online at http://meteoritics.org

Experimental study and TEM characterization of dusty olivines in chondrites: Evidence for formation by in situ reduction

Hugues LEROUX[1]*, Guy LIBOUREL[2], Laurence LEMELLE[3], and François GUYOT[4]

[1]Laboratoire de Structure et Propriétés de l'Etat Solide -ESA 8008, Université des Sciences et Technologies de Lille, F-59655 Villeneuve d'Ascq-Cedex, France
[2]Centre de Recherches Pétrographiques et Géochimiques-CNRS, BP20, F-54501 Vandoeuvre les Nancy, France, and Ecole Nationale Supérieure de Géologie-INPL, BP40, F-54501 Vandoeuvre les Nancy, France
[3]Laboratoire des Sciences de la Terre - Ecole Normale Supérieure - UMR 5570, 46 allée d'Italie, F-69364 Lyon, France
[4]Laboratoire de Minéralogie-Cristallographie and Institut de Physique du Globe de Paris - UMR 7590, Tour 16, Case 115, 4 place Jussieu, F- 75252 Paris 05, France
*Corresponding author. E-mail: hugues.leroux@univ-lille1.fr

(Received 26 October 2001; revision accepted 31 October 2002)

Abstract–An analytical transmission electron microscopy (ATEM) study was undertaken in order to better understand the formation conditions of dusty olivines (i.e., olivines containing abundant tiny inclusions of Fe-Ni metal) in primitive meteorites. Dusty olivines from type I chondrules in the Bishunpur chondrite (LL3.1) and from synthetic samples obtained by reduction of San Carlos olivines were examined. In both natural and experimental samples, micron size metal blebs observed in the dusty region often show preferential alignments along crystallographic directions of the olivine grains, have low Ni contents (typically <2 wt%), and are frequently surrounded by a silica-rich glass layer. These features suggest that dusty olivines are formed by a sub-solidus reduction of initially fayalitic olivines according to the following reaction:

$$Fe_2SiO_{4\ \text{in olivine}} = 2Fe_{\ \text{metal}} + xSiO_{2\ \text{in melt}} + (1-x)\ SiO_{\text{in gas}} + (3-x)/2O_{2\ \text{in gas}}$$

Some volatilization of SiO_{gas} may account for the apparent excess of metal relative to silica-rich glass observed in both experimental and natural samples. Comparison with experimentally produced dusty olivines suggests that time scales of the order of minutes usually inferred for chondrule formation are also adequate for the formation of dusty olivines. These observations are in agreement with the hypothesis that at least part of the metal phase in chondrites originated from reduction during chondrule formation.

INTRODUCTION

The common presence of Fe-Ni metal in the matrix and chondrules of primitive chondrite meteorites is indicative of reducing conditions in the solar nebula. However, whether chondritic metal results from equilibrium condensation in the nebula (Grossman and Olsen 1974) and/or reflects reduction processes during chondrule formation (Scott and Taylor 1983) is still a matter of debate. These issues are of fundamental importance for understanding the processes responsible for chondrule formation and metal segregation in the early solar system. Unequilibrated, ordinary chondrites preserve several categories of metal phases formed during solar nebula processes and are therefore of particular interest in addressing this problem.

In addition to spheroidal Fe-Ni metal grains, magnesian chondrules (Type I) in unequilibrated chondrites frequently contain FeO-poor olivine grains riddled with μm-sized Fe metal blebs (Rambaldi, Sears, and Wasson 1980; Rambaldi 1981; Nagahara 1981; Rambaldi and Wasson 1982; Rambaldi et al. 1983; Kracher, Scott, and Keil 1984; Jones 1996). These metallic inclusions are located in the cores of coarse olivine grains of forsteritic composition, giving a characteristic "dusty" appearance to the olivines (Fig. 1). Such dusty cores are commonly surrounded by clear olivine rims, similar in composition to normal grains of the host chondrules (e.g., Rambaldi and Wasson 1982; Jones 1996; Jones and Danielson 1997). The tiny metal blebs within olivines are poorer in Ni than the more abundant spherical metal grains present in chondrule interiors (Rambaldi and Wasson 1981). The

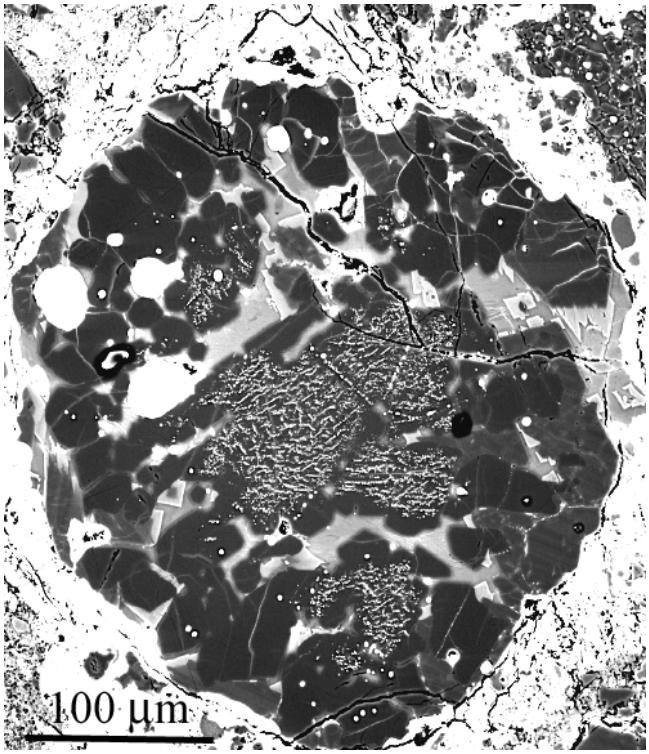

Fig. 1. SEM micrograph of a chondrule containing dusty olivines in the Semarkona chondrite (secondary electrons). Numerous metal precipitates are visible, particularly in olivine, and are located at the chondrule center.

occurrences of both metallic blebs and FeO depletion in olivine have been interpreted as the result of a solid state reduction of more ferroan olivines (Boland and Duba 1981; Rambaldi 1981; Nagahara 1981; Rambaldi and Wasson 1982; Rambaldi et al. 1983; Connolly et al., 1994; Libourel and Chaussidon 1995; Jones 1996; Jones and Danielson 1997). Recently, Lemelle et al. (2000) confirmed this idea and proposed that the formation of dusty olivines could be explained by a coupled reduction/volatilization reaction. The occurrences of dusty olivine in chondrules could indeed reflect both changes in redox conditions of the nebular gas (Nahagara 1981) and the presence of reducing agents in chondrule precursors, such as carbon (Connolly et al. 1994; Libourel and Chaussidon 1995; Hanon, Robert, and Chaussidon 1998), carbonaceous matter, or hydrogen which has been implanted by solar wind (Rambaldi and Wasson 1982). However, despite numerous studies devoted to dusty olivines, the cause of the reduction has never been clearly demonstrated.

It is commonly assumed that dusty olivines are "relict" grains in the sense that they did not crystallize in situ from the host chondrule and are unrelated to the melt of the chondrules in which they occur, as outlined by Jones and Danielson (1997). However, the origin of these peculiar grains remains a matter of debate. They may originate either from previous generations of chondrules that were recycled under reducing conditions, but survived melting in the last chondrule forming event in which they are now enclosed (Nahagara 1981; Rambaldi 1981; Rambaldi and Wasson 1982; Steele 1986; Wasson 1993; Weisberg and Prinz 1996; Rubin and Krot 1996; Jones 1996), or they could be pristine condensates in the solar nebula (Grossmman et al. 1988), or pre-solar grains of the interstellar medium. After a detailed study of the minor element contents of olivines, Jones and Danielson (1997), favor a chondrule reprocessing origin and outline the importance of chondrule recycling in chondrule formation processes.

Hence, dusty olivines, as relict grains, are of particular interest, because they may provide new constraints on chondrule formation and reprocessing events, i.e., timescales and redox conditions of thermal events in the solar nebula. However, before using these minerals as a tool for deciphering the relative chronology between reduction processes and chondrule formation events, a better understanding of the reduction processes leading to metal-silicate segregation in olivines is essential. Therefore, one of the main goals of this study is to provide new microstructural observations and chemical data, using analytical transmission electron microscopy (ATEM), on both dusty olivines in natural chondrules and in experimentally reduced olivines.

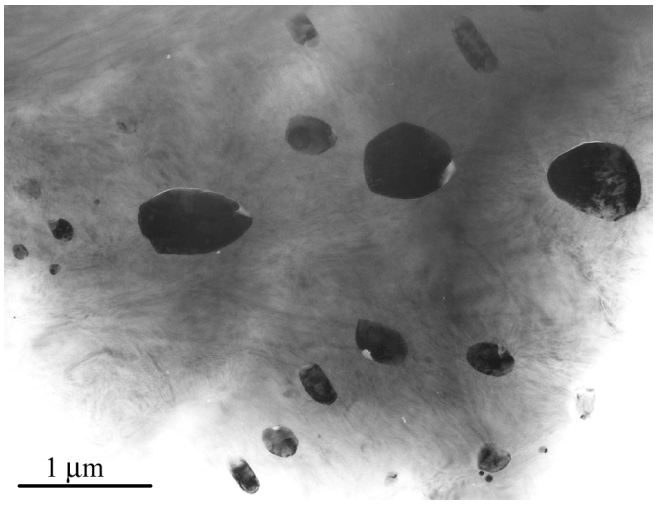

Fig. 2. A general view of a dusty region of an olivine grain containing a high density of metal blebs (TEM bright field micrograph, Bishunpur). Note the preferential alignment of some of these grains.

Table 1. Representative compositions of some metal blebs in dusty olivine in the Bishunpur sample (EDS-TEM, data in wt%). For a given analysis, the standard deviation for EDS-TEM errors on these results is 1σ.

Fe	Ni	Co
97.2 ± 1.1	1.78 ± 0.21	1.04 ± 0.29
97.3 ± 1.1	2.05 ± 0.35	0.68 ± 0.25
99.2 ± 0.7	0.35 ± 0.10	0.43 ± 0.20
98.8 ± 1.1	0.84 ± 0.15	0.34 ± 0.21
99.2 ± 1.1	0.16 ± 0.15	0.59 ± 0.30

SAMPLES AND EXPERIMENTAL PROCEDURE

Reduction processes were documented in chondrules of the Bishunpur (LL3.1) ordinary chondrite and in San Carlos olivines. The Bishunpur chondrite is one of the most unequilibrated ordinary chondrites containing essentially unaltered chondrules with pristine nebular signatures (Rambaldi and Wasson 1981). The San Carlos olivines were annealed at a high temperature, below their melting point, and at low oxygen fugacity.

Bishunpur Samples

Dusty olivines were selected using optical microscopy. All selected grains were located in low-FeO type I chondrules, having porphyritic olivine or olivine-pyroxene textures. While abundant metal grains may occur at silicate grain boundaries or are embedded in the glassy mesostasis of chondrules, we studied only metal enclosed in dusty olivines.

Experimentally Reduced Samples

For reduction experiments, San Carlos olivines, $(Mg_{0.84}Fe_{0.16})_2SiO_4$ with trace amounts of Ni, Co, P, Mn, and Ca, were used as starting material. These olivines are indeed good proxies of relict olivine grains in chondrules of unequilibrated chondrites because their composition is close to the composition of dusty olivines prior to reduction (Jones and Danielson 1997). Olivines were crushed and sieved to 50–100 μm in order to obtain grain sizes comparable to those of typical chondrule olivines. About 20 to 30 mg of olivine powder was placed in a pure graphite crucible and heated in a 1 atm vertical gas mixing furnace at 1610°C under reduced atmosphere (1700°C GERO HTVR 70-250, CRPG-CNRS, Nancy). The sample crucible was placed in the hot spot of the furnace using an alumina rod equipped with a $PtRh_{10}$-Pt thermocouple. Pure CO gas was fed to the furnace using a Tylan mass flow controller at a flow rate of 300 cm^3 min^{-1}. The oxygen fugacity was then buffered at the C/CO buffer curve, i.e., log fO_2 = –15.2 atm and 1610°C. Each experiment was terminated by drop quenching the sample at room temperature in the furnace atmosphere. The calculated equilibrium oxygen fugacity for Fe metal precipitation from $(Mg_{0.84}Fe_{0.16})_2SiO_4$ is log fO_2 = –9.94 atm at 1610°C, according to Nitsan (1974) and to updated thermodynamic models (Matas et al. 2000). Under the experimental conditions of 1610°C and log fO_2 = –15.2 atm, the Fa content of the olivine is calculated to be equal to 3.7 10^{-2}. This indicates that the selected conditions are appropriate for metal extraction from the Fa_{16} olivine. In order to simulate generation of dusty olivines at time scales relevant to chondrule formation, reduction experiments were performed during 5- and 100-minute runs (hereafter labelled R5 and R100, respectively).

Analytical Procedures

Samples were first studied by optical microscopy and scanning electron microscopy (SEM). Run products of reduction experiments were analyzed using an electron microprobe (CAMECA SX50, Nancy). For ATEM characterization, 20–30 μm thick sections were taken from selected areas of the natural or synthetic samples and polished on both sides. In the second step, these samples were thinned to electron transparency by argon ion bombardment at 5 kV acceleration voltage (<0.5 μm). Finally, the samples were coated with an approximately 30 nm thick carbon layer. Microstructural observations and X-ray microanalyses were carried out using a Philips CM30 TEM operating at 300 kV (Lille). The TEM was equipped with an energy-dispersive spectrometer (EDS Tracor-Voyager) composed of a Ge detector and an ultra-thin window. This configuration allows the detection and quantification of light elements; the O-K emission line is detected with a very good sensitivity. The Cliff and Lorimer factors (Cliff and Lorimer 1975), which depend on the characteristics of the EDS system, were determined by the parameterless extrapolation method of Van Cappellen (1990) using standard specimens of known and homogeneous compositions. Quantitative microanalyses require precise knowledge of the thickness of the analyzed areas in order to apply absorption corrections. Indeed, due to the low energy (523 eV) of the O-K line, the emitted photons undergo strong absorption. Therefore, the correct oxygen concentration strongly depends on the precise knowledge of the thickness of the analyzed area. We used the absorption correction method developed by Van Cappellen and Doukhan (1994) for silicate phases. The thickness of the analyzed area is deduced from the EDS spectra by balancing the oxygen concentration with those of cations. The sample thickness is adjusted until electroneutrality is reached by the quantification program. This method yields precise and reproducible results consistent with rules of cation site

Table 2. Representative compositions of olivine, in which metal blebs are enclosed in the Bishunpur sample (EDS-TEM, data in wt%).

SiO_2	MgO	FeO	CaO	MnO	Cr_2O_3	% Fa
41.7 ± 0.6	53.4 ± 0.6	3.9 ± 0.2	0.33 ± 0.09	0.31 ± 0.05	0.37 ± 0.08	3.9
42.0 ± 1.1	51.7 ± 0.9	5.7 ± 0.4	0.05 ± 0.04	0.38 ± 0.14	0.22 ± 0.15	5.6
41.9 ± 0.8	54.5 ± 0.9	2.6 ± 0.2	0.47 ± 0.13	0.28 ± 0.20	0.22 ± 0.06	2.5
41.5 ± 1.0	50.3 ± 1.0	7.2 ± 0.5	0.11 ± 0.09	0.14 ± 0.10	0.66 ± 0.29	7.3
42.1 ± 0.9	55.7 ± 0.9	1.3 ± 0.2	0.14 ± 0.10	0.39 ± 0.16	0.37 ± 0.20	1.3

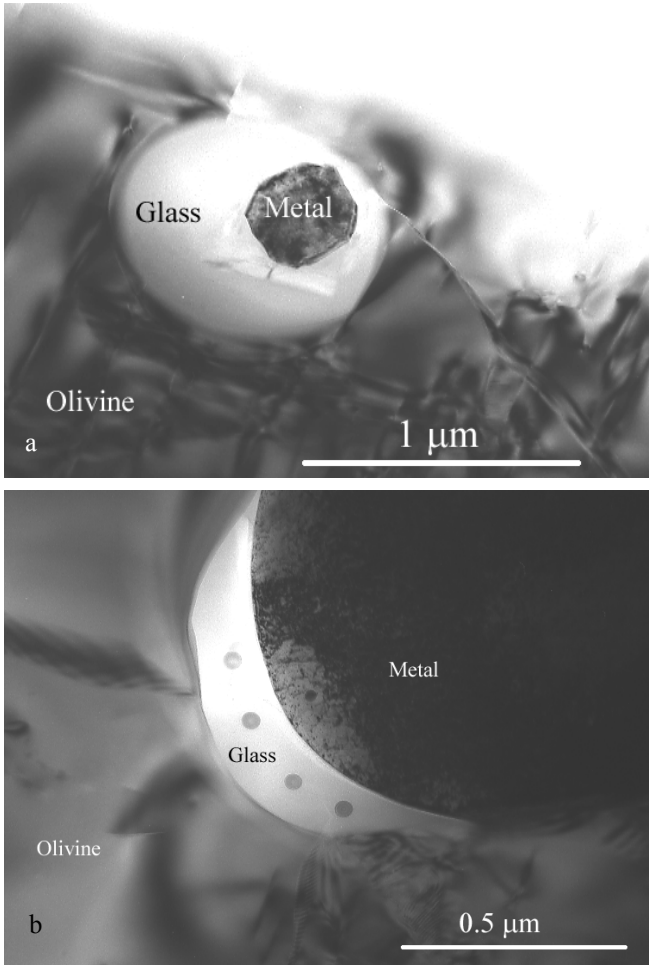

Fig. 3. TEM bright field micrographs, Bishunpur sample: a) metallic precipitates in olivine are frequently embedded in a silica-rich glass; b) large metal particle surrounded by a thin layer of silica-rich glass. The dark spots correspond to contamination strains that formed during the analysis of the glass.

occupancy. The relative errors based on counting statistics are ≈2% for major elements. To minimize the loss of volatile species under the elctron beam, glasses were analyzed with a low beam current density. For the absorption correction in metal, we experimentally calibrated the intensity ratio FeL/FeK versus the direct measurements of the thickness in a sample of pure iron.

RESULTS

Dusty Olivines from Bishunpur

According to previous findings (Rambaldi and Wasson 1982; Jones and Danielson 1997), dusty olivines contain a high density of fine metal inclusions, and these "dusty regions" are surrounded by rims of clear Mg-rich olivine.

Fig. 2 shows a typical microstructure of metallic blebs within a dusty olivine grain on the TEM scale. The diameter

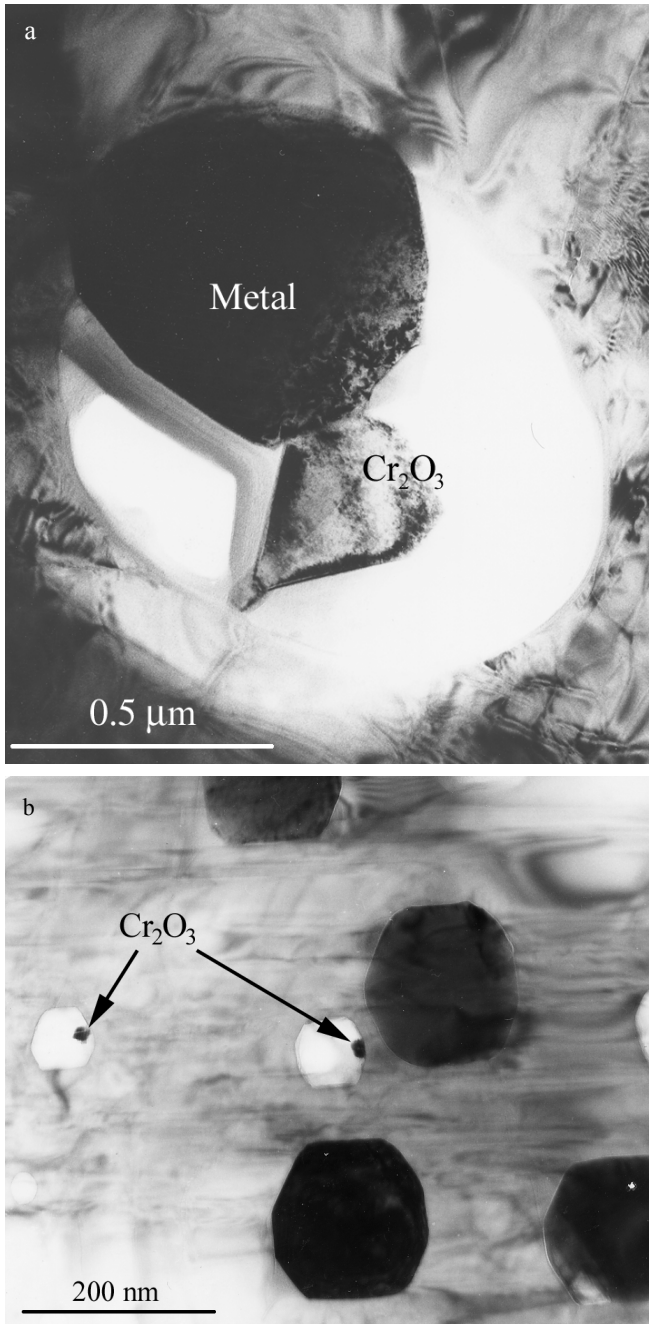

Fig. 4. TEM bright field micrographs, Bishunpur sample: a) association of metal-silicate glass and Cr_2O_3. The silicate glass, which appears in white, has been partially removed during the thinning process; b) tiny Cr_2O_3 particles (arrowed) associated with metal blebs. They are seen when metal particles are removed during the sample preparation.

of the metal globules is generally <1 μm, but ranges from 0.1 μm to 10 μm. Electron diffraction shows that the blebs consist of single crystals with body centered cubic (bcc) structure. The metal blebs have generally rounded boundaries but, in some cases, they exhibit euhedral shapes, with (110) metal parallel to (100) olivine. Occasionally, the metal blebs are

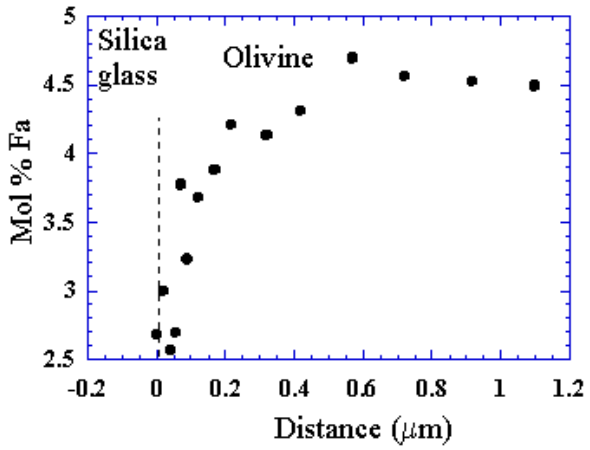

Fig. 5. Fayalite content of the olivine near a metal/glass globule of 1 μm in diameter (Bishunpur sample). Note the sharp decrease of the Fa content of the olivine at the olivine/glass boundary.

aligned along crystallographic directions, as previously observed by Jones and Danielson (1997) in chondrules and in experimentally reduced olivine (Boland and Duba 1981, 1986; Lemelle et al. 2000). Their alignment along a preferred orientation corresponds to the trail of the (100) olivine plane. The euhedral shapes as well as preferential alignments suggest a crystallographic control on the metal nucleation and growth processes.

As already noticed in previous studies (e.g., Rambaldi and Wasson 1982), the amount and composition of the metal precipitates may vary from one olivine grain to another, probably reflecting local variations in temperature, oxygen fugacity, reduction duration, and/or variability in the initial olivine composition prior to reduction. From grain to grain, the composition of metal blebs inside the same dusty region of olivines can be highly variable. The precipitates are Ni-poor Fe-Ni grains, with Ni contents ranging from 0.1 to 3.2 wt%, but typically below 1 wt%. Tables 1 and 2 show representative compositions of the metal blebs and of the olivine in which they are enclosed. The cobalt content of the blebs is also low (<1 wt%) and tends to be positively correlated with Ni. Neither chromium nor silicon were detected in these grains. The ATEM study reveals that the metal in Bishunpur dusty chondrule olivines is generally more enriched in Ni and Co than previously measured by the electron microprobe (Rambaldi and Wasson 1982).

An important finding of this study is that metal blebs in dusty olivines are often surrounded by a silica-rich glass layer (Figs. 3a, b). The metal/glass ratio is variable even within a single dusty olivine grain. In some cases, metal spheres are entirely surrounded by glass (Fig. 3a). Cutting effects in the TEM sample might partly account for the high variability of the metal/glass ratio. Owing to the small spot sizes of ATEM (≈5 nm) and the small thickness of samples (e.g., 100 nm), we were able to analyze the glass composition associated with

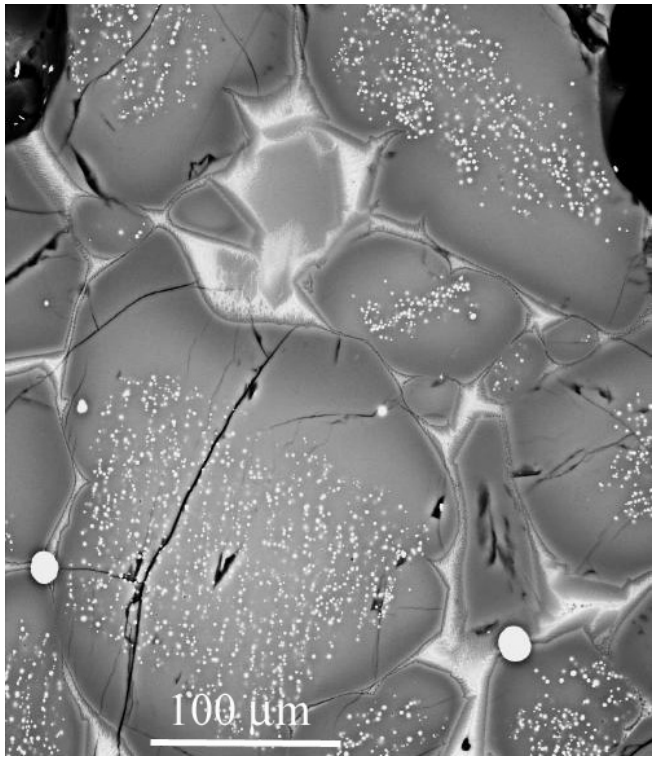

Fig. 6. The reduction experiments produced an assemblage of Fo-rich olivine, silicate glass, and metal (SEM BSE micrograph, sample R5). The metallic phases are present as tiny blebs (<1 μm) included in olivine and as globules (1 to 50 μm) located in the glass matrix at the olivine grain boundaries.

several metal blebs in different dusty olivines (Table 3). The glass is iron-poor (0.3<FeO<3 wt%) and highly variable in silica (from ≈48 up to ≈70 wt% SiO_2). The glass also contains variable amounts of Al_2O_3, CaO, and TiO_2 with concentrations as high as 28, 20, and 1 wt%, respectively. Only trace amounts of sodium and chromium were recorded.

Minor amounts of other phases were also recognized in association with the metal blebs and/or the surrounding glass (Figs. 4a, b). Because of their small sizes and their interactions with the surrounding matrix during microanalysis, we were unable to obtain detailed compositions of these phases. However, it can be shown that they are rich in Cr, P, and Ca, allowing us to identify them as chrome-III oxide (Cr_2O_3), and possibly Ca-phosphates and Ca-rich pyroxenes. The presence of Cr_2O_3 and pyroxene has also been confirmed by electron diffraction. As illustrated in Fig. 4a, some of these phases are located within the glass. In addition, compositional gradients are detected in olivines around some metal/glass globules, showing a decrease of the fayalite concentration towards the SiO_2-rich glass/olivine interface (Fig. 5).

Experimentally Reduced Olivines

Reduction experiments of San Carlos olivines with Fa_{16} yielded assemblages of Fo-rich olivine, interstitial glass, and

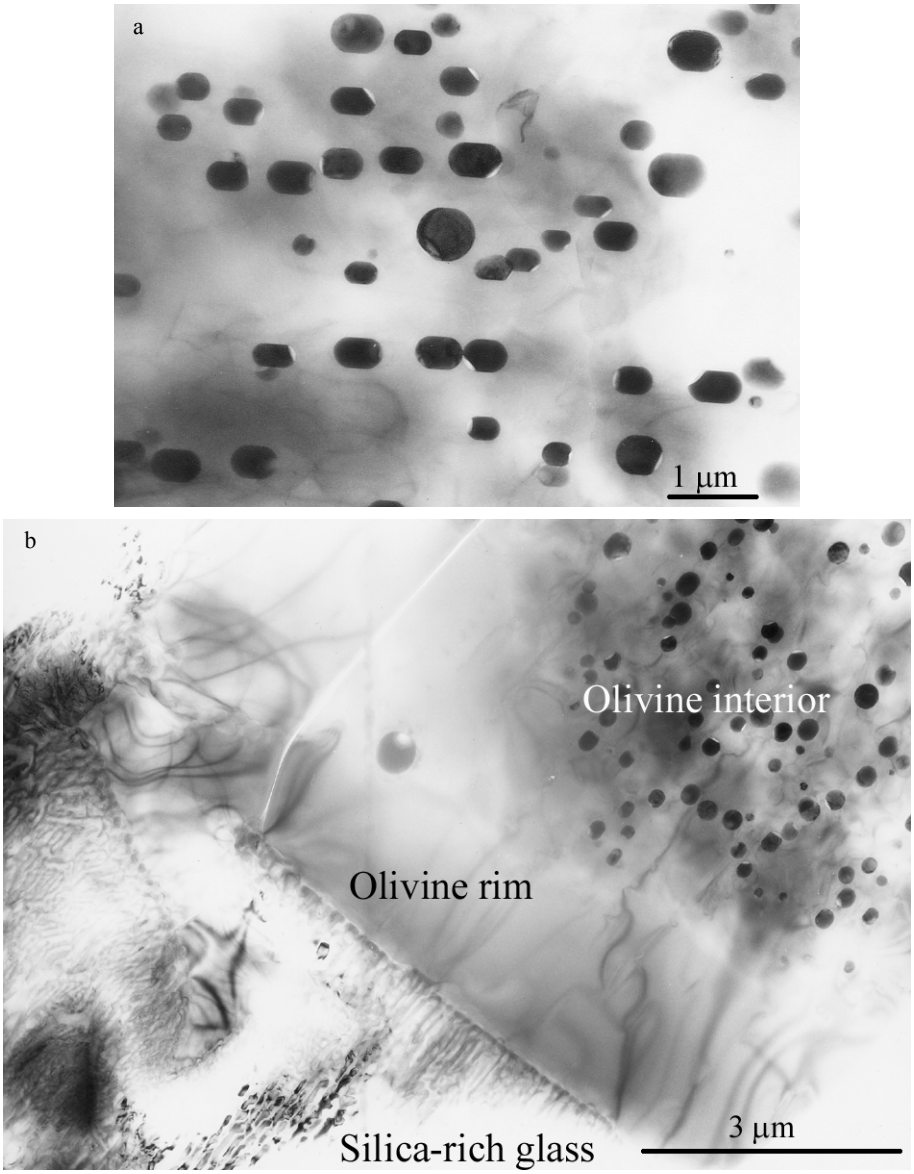

Fig. 7. TEM bright field micrographs, R100 sample: a) general view of a dusty area from an experimentally reduced San Carlos Fa16 olivine. Note the preferential orientation of the metal blebs in the olivine matrix; b) edge of an olivine grain. The rim is free of metallic precipitates. The adjacent phases to the olivine consists now of a dendrite-glass intergrowth; see text for explanation.

metal (Fe-Ni). The metal phase is present either as tiny blebs (<1 μm) embedded in olivine, mimicking natural dusty olivines, or as large globules (1 to 50 μm) located in the glass matrix at the olivine grain boundaries (Fig. 6). On the SEM scale, these textural features are very similar to those observed in the dusty olivine of type I chondrules in Bishunpur or in FeO-poor chondrules in other unequilibrated ordinary chondrites (Rambaldi and Wasson 1981, 1982; Jones and Danielson 1997).

Our ATEM study confirms that the experimentally reduced olivines (R5 and R100) are dusty and contain numerous submicrometer-sized metallic precipitates (Fig. 7a) in their core regions (Fig. 7b). The metal blebs are generally distributed randomly in the olivine matrix and sometimes show preferential alignments along the (100) plane of the olivine host. The average size of the precipitates increases with reduction duration (Fig. 8), with an average of 270 nm and 350 nm after 5 (sample R5) and 100 (sample R100) minutes of reduction, respectively. Although highly variable, the composition of the Fe metal and olivine in the dusty regions changes according to the reduction duration (see Tables 4 and 5 for representative analyses). In sample R5, Ni contents range from 1.5 to 4 wt%, with an average of 2.8 wt% (25 analyses). In sample R100, the metal composition varies from almost Ni-free to 3.2 wt% Ni and 0.2 to 2.7 Si, with an average of 1.3 Ni and 1.1 Si (21 analyses). In both runs, the Co concentrations in dusty metal were always less than 1 wt%, with mean values of 0.4 and 0.35 for R5 and R100 samples,

Table 3. Representative compositions of the SiO_2-rich glass associated to the metal blebs in the Bishunpur sample (EDS-TEM, data in wt%). Some minor amounts of Mn and K were also detected (<0.05 wt%)

SiO_2	Al_2O_3	CaO	Na_2O	FeO	MgO	Cr_2O_3	TiO_2
48.0 ± 1.2	28.4 ± 1.1	19.3 ± 0.4	0.5 ± 0.3	1.3 ± 0.1	0.87 ± 0.23	0.59 ± 0.16	0.97 ± 0.14
68.8 ± 1.2	18.7 ± 2.0	9.0 ± 0.3	n.d.	1.1 ± 0.1	1.9 ± 0.3	0.20 ± 0.11	0.34 ± 0.09
53.2 ± 0.9	27.2 ± 1.3	7.3 ± 0.3	1.0 ± 0.7	2.8 ± 0.3	8.2 ± 0.4	n.d.	0.23 ± 0.15
60.2 ± 1.4	27.8 ± 2.5	10.4 ± 0.4	n.d.	0.35 ± 0.13	1.1 ± 0.3	0.19 ± 0.15	0.16 ± 0.13
68.6 ± 1.5	25.3 ± 2.3	0.88 ± 0.21	0.5 ± 0.3	2.3 ± 0.3	1.6 ± 0.3	0.39 ± 0.21	0.41 ± 0.22

n.d. = not detected

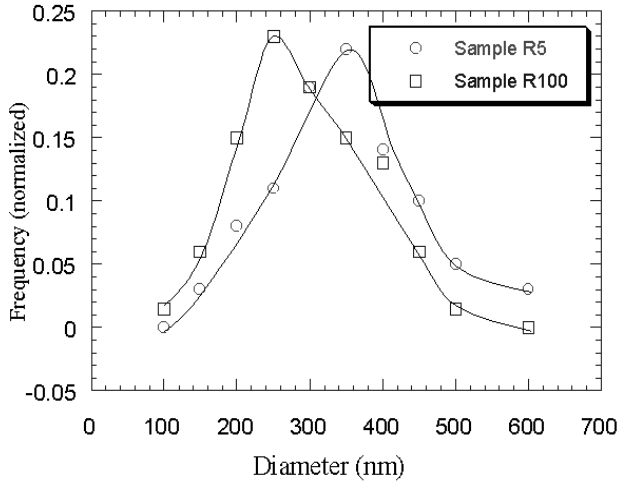

Fig. 8. Size distribution of the metallic globules in the two synthetic samples R5 and R100 showing that the globule size increase with experiment duration.

respectively. Average compositions of the larger Fe-Ni globules seated in the glass matrix at the olivine grain boundaries obtained by electron microprobe analyses are also given for comparison in Table 6. They are, on average, more Ni-rich than the metallic blebs present within the dusty olivines.

In these synthetic dusty olivines, metal phases are associated with SiO_2-rich glassy phases (Figs. 9a, b), even if these latter are less abundant than in Bishunpur chondrules. Unfortunately, the sizes of glass pockets were too small for obtaining analyses devoid of any contamination by the olivine matrix. Nevertheless, it can be shown that the glass is enriched in Al_2O_3 and CaO. Our TEM study also reveals the existence of features of coalescence between metallic precipitates (Fig. 10a) and between the glassy areas of two metal–glass globules (Fig. 10b), suggesting that coalescence is an efficient mechanism to grow larger metallic precipitates. Similar observations were made by Roeder (1981) in olivine crystals isolated from the Murchison chondrite. These crystals contained opaque spherules of Fe metal, some associated with glass, and some connected by fillets of glass. As shown in Fig. 11a, the host olivine contains dislocations, which are probably related to the growth of the metallic precipitates. In other cases, dislocation loops are also observed around the

Table 4. Representative compositions of some metal precipitates in dusty olivine experimentally reduced (EDS-TEM, data in wt%).

Fe	Ni	Co	Si
Sample R5			
96.4 ± 0.8	3.32 ± 0.18	0.31 ± 0.21	n.d.
96.9 ± 0.7	2.70 ± 0.23	0.43 ± 0.32	n.d.
98.4 ± 1.3	1.33 ± 0.22	0.34 ± 0.25	n.d.
Sample R100			
96.0 ± 1.1	2.9 ± 0.38	0.46 ± 0.29	0.67 ± 0.13
95.6 ± 0.8	1.61 ± 0.14	0.24 ± 0.22	2.54 ± 0.29
99.4 ± 1.0	0.06 ± 0.05	0.26 ± 0.22	0.24 ± 0.12

n.d. = not detected

precipitates (Fig. 11b). In this latter case, one can see that the metal bleb and the melt pool are almost separated.

The composition of olivine surrounding metallic precipitates, although depleted in iron compared to the Fa_{16} starting composition, is strongly dependent on the run duration. In sample R5, the fayalite content ranges from Fa_9 to Fa_4 (Table 5), with an average composition of $Fa_{5.8}$ (21 analyses), whereas in sample R100, the composition of the entire olivine is homogeneous and almost pure forsterite with $Fa_{0.1}$. The rims of the olivine grains are free of precipitates (Fig. 7b) and display a marked compositional gradient with the Fa content decreasing toward the edge of the grains (Fig. 12). On average, the intersititial glass between olivine grains is silica-rich (Table 7). Its composition depends, however, on the duration of the reduction run. For the short reduction time (R5), the glass is iron-rich and CaO, Al_2O_3, and TiO_2-poor, while for the longer duration (R100), the melt is iron-poor and enriched in CaO, Al_2O_3, and TiO_2. During quenching, the molten material extracted from the olivines, SiO_2-rich liquid and metal, crystallized and formed, at olivine grain boundaries, intergrowths of Fa-rich olivine dendrites with Ca, Al, Si-rich interstitial glass in variable proportions (Fig. 13, Table 5).

DISCUSSION

The TEM investigation of dusty olivines in both type I chondrules of Bishunpur and experimentally reduced San Carlos olivine samples unambiguously demonstrates that metal blebs originated from an internal reduction process of

TABLE 5. Representative compositions of olivine with metal blebs enclosed and representative compositions of the dendrite arms (EDS-TEM, data in wt.%).

SiO_2	MgO	FeO	CaO	MnO	mol % Fa
Sample R5					
42.3 ± 0.8	51.7 ± 0.7	5.8 ± 0.4	0.11 ± 0.08	0.13 ± 0.9	5.9
42.6 ± 0.7	52.7 ± 0.6	4.5 ± 0.3	0.05 ± 0.04	0.14 ± 0.10	4.5
40.4 ± 0.8	50.5 ± 0.7	8.8 ± 0.5	0.05 ± 0.04	0.17 ± 0.11	8.9
Sample R100					
42.9 ± 0.9	56.8 ± 0.7	0.14 ± 0.09	0.17 ± 0.09	n.d.	0.14
42.9 ± 0.7	56.6 ± 0.6	0.36 ± 0.15	0.17 ± 0.07	n.d.	0.35
42.8 ± 0.7	56.7 ± 0.6	0.29 ± 0.14	0.20 ± 0.09	n.d.	0.28
Dendrites (sample R5)					
39.1 ± 1.2	42.8 ± 1.4	17.3 ± 1.1	0.12 ± 0.10	0.55 ± 0.21	18.4
39.4 ± 0.9	39.3 ± 0.7	20.5 ± 1.2	0.08 ± 0.06	0.74 ± 0.25	22.5
37.6 ± 0.8	40.1 ± 0.7	21.5 ± 1.2	0.12 ± 0.08	0.70 ± 0.25	23.0

n.d. = not detected

Table 6. Average composition of large metal globules located in interstitial glass between olivine grains in reduction runs R5 and R100, obtained by EMPA.

	Fe	Co	Ni	Si
Sample R5				
mean[a]	94.95	0.41	5.52	n.d.
1σ	1.60	0.13	1.42	–
Sample R100				
mean[a]	92.59	0.22	2.69	1.73
1σ	2.24	0.06	0.77	0.92

[a]Average of 10 to 15 analyses of different metal blebs
n.d = not detected

olivines. The strongest arguments are provided by the close associations between metal and silica-rich glass and by the numerous intimate crystallographical relationships between metal and olivine crystals. Formation of dusty olivines were hitherto accounted for by the two following reduction reactions formulated by Nitsan (1974):

$$Fe_2SiO_{4\ in\ olivine} = 2Fe_{\ in\ metal} + SiO_{2\ in\ silica} + O_{2\ in\ gas} \quad (1)$$

$$Fe_2SiO_{4\ in\ olivine} = Fe_{\ in\ metal} + FeSiO_{3\ in\ orthopyroxene} + O_{2\ in\ gas} \quad (2)$$

However, our present investigations clearly show that the silica-rich reaction products are neither a silica polymorph nor a pyroxene, but a silica-rich melt, suggesting that the most likely reduction reaction is the following:

$$Fe_2SiO_{4\ in\ olivine} = 2Fe_{\ in\ metal} + SiO_{2\ in\ melt} + O_{2\ in\ gas} \quad (3)$$

Accordingly, this mechanism of metal segregation leads to the depletion of FeO in the adjacent olivine and involves Fe-Mg interdiffusion in olivine, as already observed by Libourel and Chaussidon (1995) and by Lemelle et al. (2000) at a lower temperature (1350°C). The process is schematically illustrated in Fig. 14.

Considering the molar balance of products in reaction (3), the volume proportion of glass should be close to twice that of metal. In both natural and experimental chondrules, however, our observations have shown that the highly variable glass to metal ratios are generally considerably lower than expected, even if we take into consideration that the glass is not composed of pure silica. Two different explanations, or their combination, may account for this observation. A first possibility is that the SiO_2-rich melt would have been preferentially transported outside the grains toward olivine grain boundaries, and thus more easily extracted from the olivine than metal, as previously suggested by Libourel and Chaussidon (1995) and illustrated in Fig. 6. This melt could subsequently be incorporated in the interstitial melt in our experiments or in the molten mesostasis in chondrules. A second possibility would be that some silicon volatilization occurred. Indeed, Lemelle et al. (2000) proposed that the formation of some dusty olivines at a lower temperature (i.e., 1350°C) could be due to a coupled reduction/volatilization reaction according to:

$$Fe_2SiO_{4\ in\ olivine} = 2Fe_{\ in\ metal} + SiO_{\ in\ gas} + 3/2\ O_{2\ in\ gas} \quad (4)$$

In this case, no silica-rich melt is expected in the reaction zone in which only olivine and metal should be observed, as shown by Lemelle et al. (2000) in their olivine single crystal reduction experiments. As silicon and oxygen diffusivities are much smaller than that of Fe-Mg interdiffusion in olivine (e.g., Chakraborty 1997), short-circuit diffusion of silicon and oxygen must occur for this mechanism to operate (Lemelle et al. 2000), very likely due to dislocations and sub-grain boundaries in olivines. This process favors the transport of these elements from bulk to the surface and makes an internal reduction reaction possible. Because olivine and metal with various (in any case low) proportions of SiO_2-rich melt have been observed in reaction zones of both natural and synthetic samples, it seems very likely that the formation of dusty

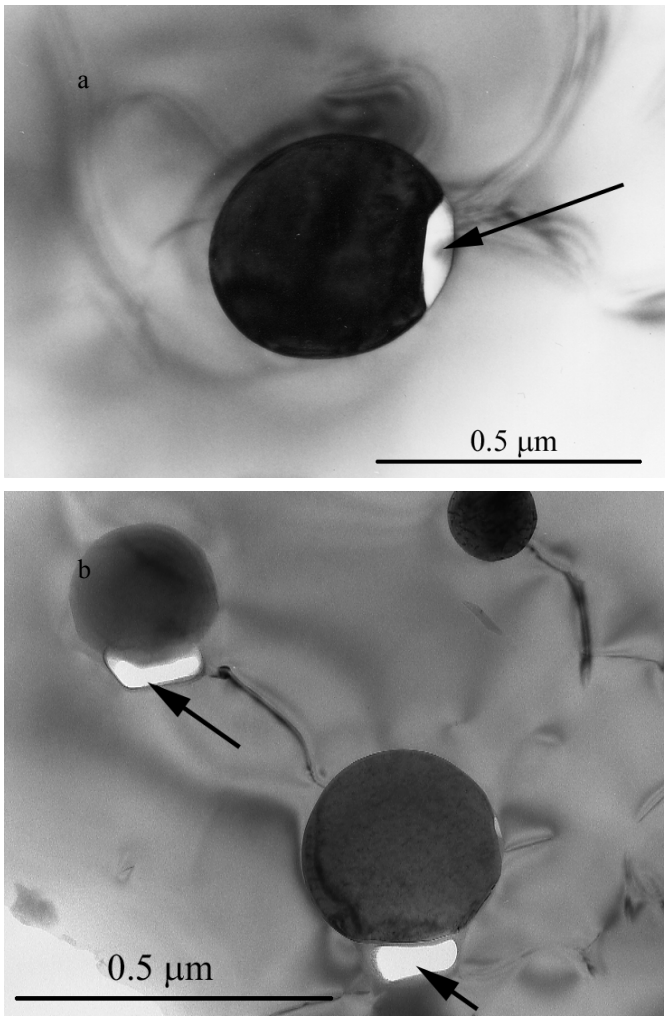

Fig. 9. TEM bright field micrographs: a) association of metal-silica-rich glass in an olivine from sample R5; b) same association in sample R100. On each figure, metal particles appear in black and the silica-rich glass pockets are arrowed.

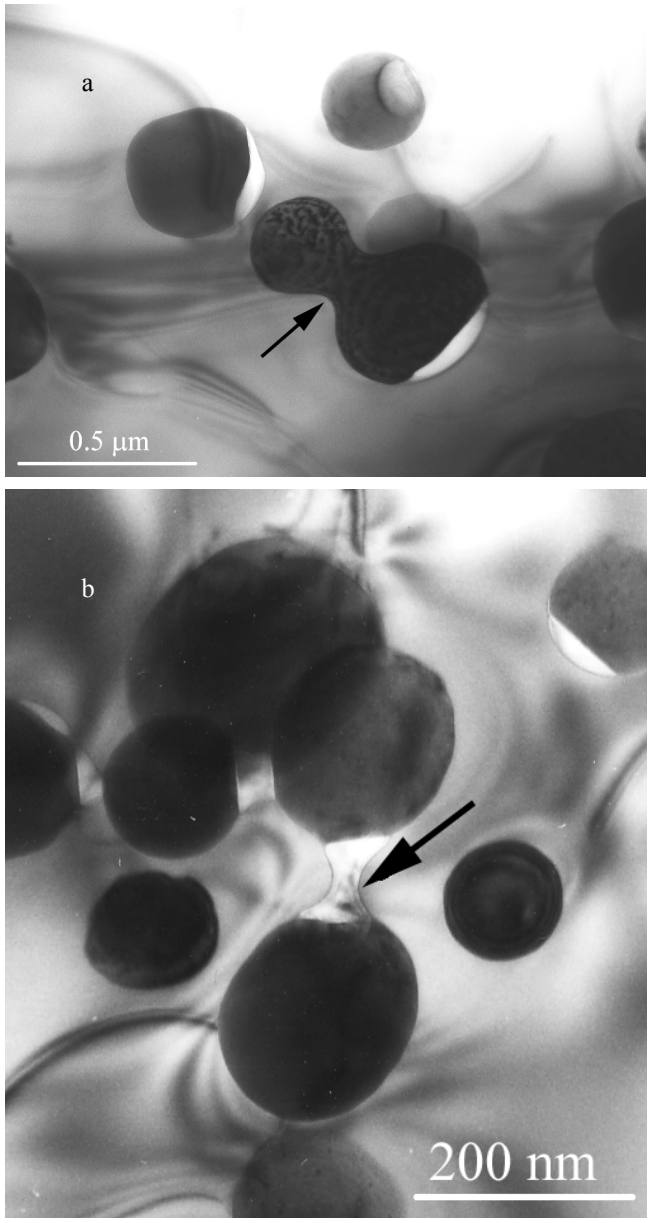

Fig. 10. TEM bright field micrographs, R100 sample: a) figures of coalescence between two metallic precipitates (arrow); b) figures of coalescence between two glassy parts of different metal/glass globules (arrow).

olivines can be explained by the coupling of reactions (3) and (4) according to:

$$Fe_2SiO_{4\ in\ olivine} = 2Fe_{\ metal} + x\ SiO_{2\ in\ melt} + (1-x)\ SiO_{\ in\ gas} + (3-x)/2O_{2\ in\ gas} \quad (5)$$

Even if the exact stoichiometry is unknown, this reaction implies the motion of only part of the oxygen and the silicon from the inside toward the outside of the olivine grains, leading to a potential depletion of silica or silicon in the dusty solid residue (extraction imposed by the low fO_2).

It is worth notice that the discrepancy in the glass/metal ratio between what was observed and what was expected could also be explained by partial reduction of the SiO_2 component of olivines into metallic Si, because Si metal will alloy with the Fe metal blebs and hence decrease the glass/metal ratio as reduction proceeds. However, this reduction reaction did not occur since the silicon concentration of metallic blebs of natural dusty olivines is always below the detection limit of our EDS system. According to our experiments (see also Libourel and Chaussidon 1995), such low silicon concentration in the metal blebs of natural dusty olivines implies, rather, that the reduction is a fast process and/or occurs at some intermediate oxygen fugacities below the IW but well above the C/CO buffer curves.

Experimentally annealed samples display olivine with precipitate-free rims. This metal precipitate configuration is also observed in the natural dusty olivine in chondrules (e.g.,

Table 7. Average composition (in wt%) obtained by EMPA of interstitial glass between olivine grains in reduction runs R5 and R100.

	Na_2O	MgO	Al_2O_3	SiO_2	K_2O	CaO	TiO_2	Cr_2O_3	MnO	FeO	mol %Fa[a]
Sample R5											
mean[b]	n.d.	11.58	3.70	56.70	n.d.	4.57	0.99	n.d.	0.86	20.10	22.6
1σ	–	4.62	1.33	1.67	–	2.56	0.46	–	0.22	1.14	
Sample R100											
mean[b]	n.d.	18.09	14.22	51.27	n.d.	13.90	2.12	n.d.	n.d.	0.76	<0.7
1σ	–	0.68	1.10	0.73	–	0.23	0.18	–	–	0.27	

[a]Calculated olivine composition in equilibrium with the silica-rich melt.
[b]Average of 5 to 10 spots.
n.d. = not detected

Jones and Danielson 1997). The metal precipitate-free zone (PFZ) adjacent to a grain boundary is frequently observed in thermally processed materials. The reason for PFZ formation is that nucleation occurs preferentially on grain boundaries which are potential nucleation sites. This phenomenon is strongly enhanced by the imposed reduced conditions. Indeed, the low oxygen fugacity tends to extract iron and oxygen from the olivines, thus making the concentration of vacancies high near the edges of the grains. This particular condition enhances the species diffusion in the rims and is also the cause of the appearance of a compositional gradient (shown on Fig. 12). Fayalite-rich dendrites in contact with these rims in R5 experiments (Fig. 13) are simply artifacts due to the rapid crystallization of the FeO-rich melt during quenching (Table 7).

Interestingly, ATEM analyses reveal that the melt composition surrounding metal blebs in dusty regions does not consist of pure silica but is diluted by elements other than Si, including some refractory elements (Table 3), very likely due to reduction of other iron-bearing olivine end-members (e.g., $CaFeSiO_4$). The highly variable character of these melts, very often in a single host olivine grain, has to be related to complex fractionation processes occurring during the reduction pulse, i.e., the duration and the efficiency of the reduction processes and/or the partial volatilisation of Si. In natural chondrules, petrological observations have revealed the occurrence of melt inclusions in olivines with highly variable compositions, from silica-poor to silica-rich, and with or without metal blebs attached to them (Roedder 1981). Owing to our experimental study, we suggest that at least some of these melt inclusions observed in chondrule olivines probably originated in such reduction mechanisms, as the melt phase can be mechanically separated from the Fe metallic blebs (see Figs.10b, 11b).

The Ni contents of the order of 1 wt% in both natural and synthetic metal particles of dusty olivines are much lower than those observed in most metallic phases of meteorites. They reflect the relatively low Ni contents of the olivine starting materials prior to reduction. This difference between normal metal from meteorites and metal inclusions in dusty olivines shows that dusty olivines were formed by reprocessing previous generations of olivines from chondrules or magmatic rocks in which olivines had already undergone Ni depletion by complete or partial equilibration with metal (Rambaldi and Wasson 1981; Jones 1996; Jones and Danielson 1997). It is also important to note that the relative heterogeneity in the composition of the Fe metallic blebs in natural dusty olivines does not necessarily imply several episodes of recycling since our experiments show that only one pulse of reduction can be responsible for such heterogeneity.

The strong similarities between the synthetic and natural dusty olivines (distribution, size, shape of the metallic particles, and presence of a SiO_2-rich glass) show that we have found appropriate conditions to experimentally simulate the formation of dusty olivines. This opens new possibilities for understanding thermally activated redox reactions which occurred in the early solar system and led to the formation of dusty olivines. Some important differences exist, however, between the synthetic and natural samples.

1. The metal particles in the Bishunpur dusty olivines contain, on average, less Ni (and Co) than those produced by experimental reduction of the San Carlos olivines. This may reflect differences between the Ni content of olivines prior to reduction and/or temperature-oxygen fugacity differences in the reduction process.
2. Fe-Mg gradients do not exist around metal blebs in synthetic dusty olivines whereas, they are occasionally observed around globules in Bishunpur. When present, however, these gradients are very sharp. For example, the quantity of iron extracted from olivine, implied by the profile shown in Fig. 5, would correspond to metal and glass spheres of about 15–20 nm where a metallic globule of ≈1 μm size is indeed observed. Such secondary Fe-Mg profiles were probably formed during one or several brief heating episodes postdating the formation of metallic globules. Alternatively, the occurence of such Fe-Mg zoning in natural samples, and their absence in synthetic samples, may be explained by their different thermal history. Our experiments are indeed isothermal and terminated by a rapid quench, and that is obviously not the case for natural samples.

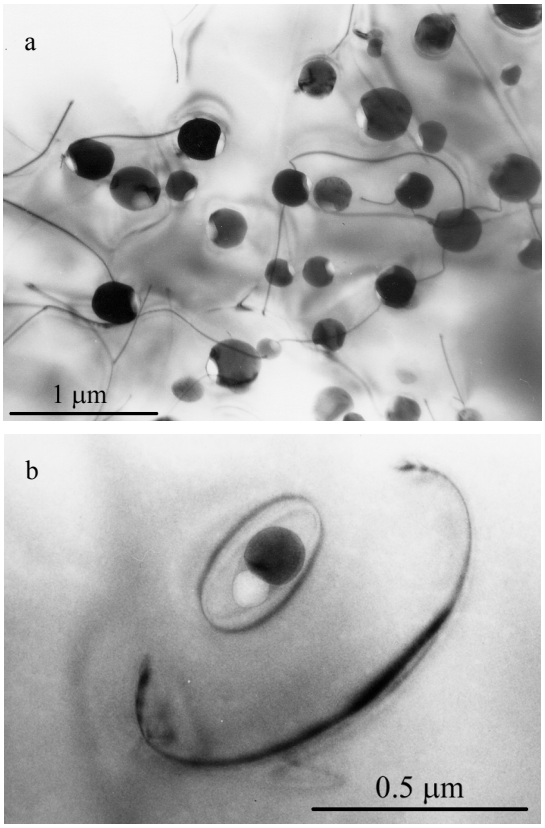

Fig. 11. TEM bright field micrographs, R100 sample: a) the dusty olivines contain some dislo cations related to the growth of the precipitates; b) two dislocation loops surrounding a metallic precipitate, illustrating the nucleation process of the dislocations.

3. Cr-III-oxide and Ca-phosphate inclusions are associated to the metal/glass particles in Bishunpur and not observed in synthetic dusty olivines. Zanda et al. (1994) have shown that most metal in primitive chondrites indeed contains small inclusions of silica, Cr_2O_3, and phosphate. They have suggested that Cr and P from the silicates were reduced into the metal during chondrule formation and afterwards reoxidized. The origin of Cr_2O_3 and phosphate particles observed in dusty olivines from Bishunpur could be similar. Cr and P from the initial olivine could have been included in the metal during reduction and subsequently reoxidized during oxidizing events. Alternatively, Cr_2O_3 and phosphates could have crystallized from the melt phase during later thermal events. In summary, the main differences between Bishunpur and synthetic dusty olivines can be understood if the natural samples have been affected by thermal events postdating the formation of the metal blebs or by a moderate cooling rate (compared to the synthetic samples), yielding very sharp Fe-Mg profiles as well as tiny Cr_2O_3 and Ca-phosphate crystals. Because these thermal events have drastic influence on the mineralogy of these objects, it would be interesting to simulate their effect in future laboratory experiments.

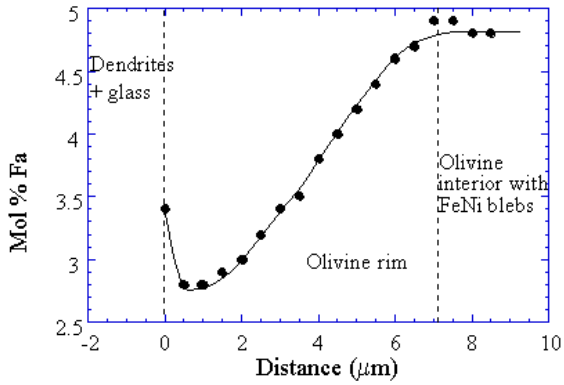

Fig. 12. Compositional gradient of olivine from core (dusty area) to edge (dendritic zone). The situation is similar to that depicted in Fig. 7b. The small increase of FeO near the rim is probably due to the quench effect (R5 sample).

Large scale microstructures in the synthetic samples also suggest that the metal-silicate differentiation mechanism in chondrites could also have been operative on a larger scale during chondrule formation. Indeed, the rims of the olivine grains in the synthetic samples are free of precipitates and display a marked Fe-Mg profile. This Fe depletion in the rim may account for the large metal grains found at olivine grain boundaries (Fig. 6). The microstructural and compositional gradients show that the reduction reaction is kinetically constrained. The driving force of the metal extraction in the rims is the low extrinsic oxygen fugacity, as well as the surface energy associated with the rims. Similar free rims and compositional gradients are also present in natural dusty olivine from chondrules (e.g., Jones and Danielson 1997). In any case, such a microstructure illustrates that metal can be formed from silicates during a chondrule reduction event at low oxygen fugacity. From texture or composition of the metal phase, a number of studies also came to this conclusion. For instance, Rambaldi and Wasson (1981) observed metal (frequently Cr and Si-rich) coalescence and expulsion textures in chondrules from Bishunpur. In a study of the very unequilibrated Semarkona chondrite, Grossman and Wasson (1987) deduced that the metal chondrule rims were derived from their interiors. Scott and Taylor (1983) suggested that the metal compositions in the least metamorphosed type 3 chondrites would reflect reduction during chondrule formation. More recently, this interpretation was reinforced by instrumental and radiochemical neutron activation analysis (Kong and Ebihara 1997), which indicates that metal in ordinary chondrites would be formed by the melting and reduction of highly oxidized material.

The reducing agent responsible for the formation of dusty olivines in Bishunpur has not been identified in our TEM investigation. It seems that carbon, the reducing agent used in our experiments, is a good candidate because it has recently been found in relatively high concentrations in

Fig. 13. Detail of the olivine dendrites (in dark) which crystallized from the melt (in bright) during the quench (TEM bright field micrograph, R5 sample). Note from Tables 5 and 7 that the fayalite content of the olivine dendrites is high.

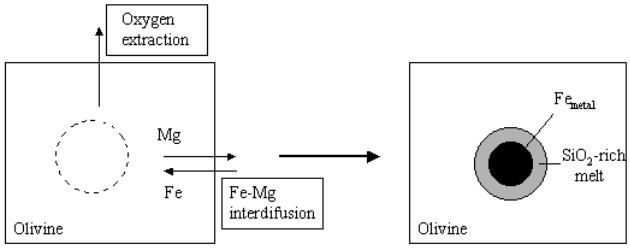

Fig. 14. Schematic representation of formation of dusty olivine by oxygen extraction and Fe-Mg interdiffusion in the olivine matrix.

silicates from highly unequilibrated chondrites (Hanon, Robert, and Chaussidon 1998), in olivines or glass inclusions in olivines of CV3 carbonaceous chondrites (Varela and Metrich 2000; Varela et al. 2000), or in metal as graphite inclusions in a number of type 3 ordinary chondrites, including Bishunpur (Mostefaoui et al. 2000; Zanda et al. 1994). In the latter case, graphite is interpreted as residual carbon that did not undergo reduction processes. Carbon present in chondrules could thus be the main reducing agent for forming dusty olivines. Several reduction experiments of olivine have been conducted in the past (Boland and Duba 1986; Connolly et al. 1994; Libourel and Chaussidon 1995; Connolly and Hewins 1996; Lemelle et al. 2000, 2001). Below the melting temperature of olivine, Fe-Ni blebs are produced within the olivine grains which progressively become forsterite-rich. Our experimental study shows that the formation of tiny metallic precipitates within an olivine matrix requires heating under reducing conditions over brief periods on the order of minutes at temperatures just below the melting point of olivine, a time scale relevant to chondrule formation. Our experimental study has also shown that the characteristics of the reduction process leading to dusty olivines including the detailed compositions of the different phases in the reduced assemblage (forsterite-rich olivine, metal, silica-rich glass) are strongly sensitive to temperature, reduction duration, and oxygen fugacity (see also Libourel and Chaussidon 1995). Further reduction experiments and detailed observations of natural dusty olivines are thus needed to provide new information about thermal events in the early solar system.

CONCLUSION

ATEM study of dusty olivines in type I chondrules of Bishunpur and in experimentally reduced San Carlos olivines leads to the following conclusions:

1. Dusty olivines form by an in situ reduction of the fayalite compound of olivine, according to the following reaction:

$$Fe_2SiO_{4\ \text{in olivine}} = 2Fe_{\ \text{in metal}} + SiO_{2\ \text{in glass}} + O_{2\ \text{in gas}} \quad (3)$$

2. The metal to glass ratio observed by ATEM has been shown to exceed the stoichiometric proportions predicted by reaction (3). This may be explained either by preferential extraction of the silica-rich melt from the olivines or by preferential volatilization of silicon monoxide. A combination of these two processes may explain the observations. Further experiments are needed for establishing their relative importance as a function of temperature, oxygen fugacity, and run duration.
3. The Ni contents of dusty olivines were measurable due to the high spatial analytical resolution of ATEM. Consistent with previous determinations by electron microprobe, the Ni contents are found to be much smaller than those observed in most metallic phases of meteorites, reflecting the relatively low Ni content of the olivine starting materials prior to reduction. This strongly argues for a formation of dusty olivines by reprocessing previous generations of chondrules (magmatic origin) in which olivines had already undergone Ni depletion.
4. The formation of dusty olivines occurs at olivine sub-solidus temperature. Otherwise, the fine metal grains in the olivine interiors would have coalesced if the olivine matrix had been molten. At the temperature of 1610°C of our experiments, the formation of dusty olivines occurs over durations of the order of minutes. These conditions

are similar to that believed to be necessary for forming chondrules.

5. The main differences between the studied experimental and natural dusty olivines are the presence of sharp Fe-Mg diffusion profiles, small chondrite particles, and Ca-phosphate associated with the metal blebs in dusty olivines. These observations are interpreted as secondary processes due to thermal events post-dating the formation of the dusty olivines.

Acknowledgments–This work was supported by the INSU-CNRS (Programme National de Planétologie). The authors thank the Muséum National d'Histoire Naturelle de Paris for providing the Bishunpur sample. A. Rouillier is thanked for assistance in the high-temperature experimental laboratory of the CRPG-CNRS. We are also grateful to A. Köhler, R. Podor, F. Diot, and S. Barda for assistance with electron microprobe analyses and SEM at the Service d'Analyses of the Université Henri Poincaré, Nancy. M. Bacia and J. F. Dhénin are thanked for their assistance in the analytical transmission electron microscope work at the Centre Commun de Microscopie of the Université des Sciences et Technologies de Lille. The authors are grateful to F. Langenhorst, A. Pack, and F. Brenker for their thorough and helpful reviews and to the MAPS associate editor A. Deutsch for his careful work.

REFERENCES

Boland J. N. and Deba A. G. 1981. Reduction of olivine in the solid state: Implications for planetary and meteoritic evolution. *Nature* 294:142–144

Boland J. N. and Deba A. G. 1986. An electron microscope study of the stability field and degree of nonstoichiometry in olivine. *Journal of Geophysical Research* 91:4711–4722

Chakraborty S. 1997. Rates and mechanisms of Fe-Mg interdiffusion in olivine at 980°C–1300°C. *Journal of Geophysical Research* 102:12317–12331.

Cliff G. and Lorimer G. W. 1975. The quantitative analysis of thin specimens. *Journal of Microscopy* 103:203–207.

Connolly H. C., Hewins R. H., Ash R. D., Zanda B., Lofgren G. E., and Bourot-Denise M. 1994. Carbon and the formation of chondrules. *Nature* 371:136–139.

Connolly H. C. and Hewins R. H. 1996. Constraints on chondrule precursors from experimental data. In *Chondrules and the protoplanetary disk,* edited by Hewins R. H., Jones R. H., and Scott E. R. D. Cambridge: Cambridge University Press. pp. 129–135.

Grossman J. N. and Wasson J. T. 1987. Compositional evidence regarding the origins of rims on Semarkona chondrules. *Geochimica et Cosmochimica Acta* 51:3003–3011.

Grossman J. N., Rubin A. E., Nagahara H., and King E. 1988. Properties of Chondrules. In *Meteorites and the early solar system,* edited by Kerridge J. F. and Mattews M. S. Tucson: University of Arizona Press. pp. 619–659.

Grossman L. and Olsen E. 1974. Origin of the high-temperature fraction of C2 chondrites. *Geochimica et Cosmochimica Acta* 38:173–187.

Hanon P., Robert F., and Chaussidon M. 1998. High carbon concentrations in meteoritic chondrules: a record of metal-silicate differentiation. *Geochimica et Cosmochimica Acta* 62: 903–913.

Jones R. H. 1996. Relict Grains in chondrules: Evidence for chondrule recycling. In *Chondrules and the protoplanetary disk,* edited by Hewins R. H., Jones R. H., and Scott E. R. D. Cambridge: Cambridge University Press. pp. 163–172.

Jones R. H. and Danielson L. R. 1997. A chondrule origin for dusty relict olivine in unequilibrated chondrites. *Meteoritics & Planetary Science* 32:753–760.

Kong P. and Ebihara M. 1997. The origin and nebular history of the metal phase of ordinary chondrites. *Geochimica et Cosmochimica Acta* 61:2317–2329.

Kracher A., Scott E. D. R., and Keil K. 1984. Relict and other anomalous grains in chondrules: implications for chondrule formation. *Journal of Geophysical Research* 89: B559–B566.

Lemelle L., Guyot F., Fialin M., and Pargamin J. 2000. Experimental study of chemical coupling between reduction and volatilization in olivine single crystals. *Geochimica et Cosmochimica Acta* 64: 3237–3249.

Lemelle L., Guyot F., Leroux H., and Libourel G. 2001. An experimental study of the external reduction of olivine single crystals. *American Mineralogist* 86:47–54.

Libourel G. and Chaussidon M. 1995. Experimental constraints on chondrule reduction (abstract). *Meteoritics* 30:536–537.

Matas J., Ricard Y., Lemelle L., and Guyot F. 2000. An improved thermodynamic model of metal-olivine-pyroxene stability domains. *Contributions to Mineralogy and Petrology* 140:73–83.

Mostefaoui S., Perron C., Zinner E., and Sagon G. 2000. Metal-associated carbon in primitive chondrites: Structure, isotopic composition, and origin. *Geochimica et Cosmochimica Acta* 64: 1945–1964.

Nagahara H. 1981. Evidence for secondary origin of chondrules. *Nature* 292:135–136.

Nitsan U. 1974. Stability field of olivine with respect to oxidation and reduction. *Journal of Geophysical Research* 79:706–711.

Rambaldi E. R., Sears D. W. G., and Wasson J. T. 1980. Si-rich Fe-Ni grains in highly unequilibrated ordinary chondrites. *Nature* 287: 817–820.

Rambaldi E. R. 1981. Relict grains in chondrules. *Nature* 293:558–561.

Rambaldi E. R. and Wasson J. T. 1981. Metal and associated phases in Bishunpur, a highly unequilibrated ordinary chondrite. *Geochimica et Cosmochimica Acta* 45:1001–1015.

Rambaldi E. R. and Wasson J. T. 1982. Fine, nickel-poor Fe-Ni grains in the olivine of unequilibrated ordinary chondrites. *Geochimica et Cosmochimica Acta* 46:929–939.

Rambaldi E. R., Rajan R. S., Wang D., and Housley R. M. 1983. Evidence for relict grains in chondrules of Qingzhen, an E3 type enstatite chondrite. *Earth and Planetary Science Letters* 66:11–24.

Roedder E. 1981. Significance of Ca-Al-rich silicate melt inclusions in olivine crystals from the Murchison type II carbonaceous chondrite. *Bulletin de Minéralogie* 104:339–353.

Rubin A. E. and Krot A. N. 1996. Multiple heating of chondrules. In *Chondrules and the protoplanetary disk,* edited by Hewins R. H., Jones R. H., and Scott E. R. D. Cambridge: Cambridge University Press. pp. 173–180.

Scott E. R. D. and Taylor G. J. 1983. Chondrules and other components in C, O, and E chondrites: similarities in their properties and origins. *Journal of Geophysical Research* 88: B275–B286.

Steele I. M. 1986. Compositions and textures variations of relict forsterite in carbonaceous and ordinary unequilibrated chondrites. *Geochimica et Cosmochimica Acta* 50:1379–1395.

Van Cappellen E. 1990. The parameterless correction method in X-ray microanalysis. *Microscopy, Microanalysis, Microstructures*

1:1–22.
Van Cappellen E. and Doukhan J. C. 1994. Quantitative transmission X-ray microanalysis of ionic compounds. *Ultramicroscopy* 53: 343–349.
Varela M. E., Metrich N., Bonnin-Mosbath M., and Kurat G. 2000. Carbon in glass inclusions of Allende, Vigarano, Bali and Kaba (CV3) olivine. *Geochimica et Cosmochimica Acta* 64:3923–3930.
Varela M. E. and Metrich N. 2000. Carbon in olivines of chondritic meteorites. *Geochimica et Cosmochimica Acta* 64:3433–3438.
Wasson J. T. 1993. Constraints on chondrule origins. *Meteoritics* 28: 14–38.
Weisberg M. K. and Prinz M. 1996. Agglomeratic chondrules, chondrule precursors, and incomplete melting. In *Chondrules and the protoplanetary disk*, edited by Hewins R. H., Jones R. H., and Scott E. R. D. Cambridge: Cambridge University Press. pp. 119–127.
Zanda B., Bourot-Denise M., Perron C., and Hewins R. 1994. Origin and metamorphic redistribution of silicon, chromium, and phosphorus in metal of chondrites. *Science* 265:1846–1849.